Rare Earth Element Adsorption to Clay Minerals: Mechanistic Insights and Secondary Source Implications

Brendan A. Bishop[a*], Md. Samrat Alam[b], Shannon L. Flynn[c], Ning Chen[d], Weiduo Hao[e,f], Karthik Ramachandran Shivakumar[f], Logan Swaren[f †], Daniela Gutierrez Rueda[f], Kurt O. Konhauser[f], Daniel S. Alessi[f], Leslie J. Robbins[a]

[a]-Department of Geology, University of Regina, 3737 Wascana Parkway, Regina, Saskatchewan S4S 0A2, Canada
[b]-Geological Survey of Canada, Natural Resources Canada, Québec, QC, G1K 9A9, Canada
[c]-School of Natural and Environmental Sciences, Newcastle University, Newcastle upon Tyne NE1 7RU, United Kingdom
[d]-Canadian Light Source Inc., University of Saskatchewan, 114 Science Place, Saskatoon, Saskatchewan S7N 0X4, Canada
[e]-State Key Laboratory of Continental Dynamics, Shaanxi Key Laboratory of Early Life and Environment, Department of Geology, Northwest University, Xi'an 710069, PR China.
[f]-Department of Earth and Atmospheric Sciences, 1-26 Earth Sciences Building, University of Alberta, Edmonton, Alberta T6G 2E3, Canada.

*Corresponding author: bab495@uregina.ca
[†] Upstream Research, Imperial Oil Resources Limited, Calgary, Alberta, T2C 5R2, Canada

Abstract

The energy transition will require significant mineral resources, and there is growing interest in recovering rare earth elements (REE) from unconventional secondary sources including those from low-temperature and sedimentary environments. Such sources include acid mine drainage and mine tailings, geothermal and formation waters, oilsands tailings, and coal and coal ashes. Extraction of secondary REE sources can have environmental and economic advantages over mining primary ore deposits, involving reusing waste or as a part of a remediation strategy, contributing to the circular economy. However, the development of exploration and recovery processes from these secondary sources are still in their infancy, and a broader understanding of the enrichment mechanisms is required before we will have the ability to identify and predict settings which best support REE extraction. Among these sources, a unifying factor is the role of clay minerals since they play a key role in the transport and deposition of REE in each of these settings.

The adsorption of three REE (Pr, Dy, and Yb) to the common clay minerals illite and kaolinite was investigated through surface complexation modelling (SCM) coupled with extended x-ray absorption fine structure (EXAFS). We found that REE adsorption was affected by pH, ionic strength, and clay mineralogy. Under acidic conditions, illite had a higher adsorption capacity than kaolinite. Adsorption increased with pH, with nearly 100% adsorption at pH ~7 regardless of ionic strength or clay type. The results were used to develop a SCM to calculate the relative adsorption affinity of REE to common surface functional groups on phases including hydrous ferric and manganese oxides, humic acid, and bacteria. The model indicated that at lower pH, humic acid and hydrous ferric oxide dominated REE speciation with clays became increasingly important from circumneutral to basic pH values. EXAFS modelling of the Y K-edge showed the presence

of both inner sphere Y-Y and Y-Si and outer sphere Y-O complexation. Together, these results demonstrate that clay minerals play a significant role in the transport and enrichment of REE in sedimentary systems.

Keywords: rare earth elements, geochemical modeling, circular economy, clay minerals, critical minerals

Introduction

The rare earth elements (REE) have traditionally been used as geological tracers since they can be fractionated by a number of geochemical and mineralogical processes (Henderson, 1984). More recently, there is significant interest in REE due to their role in clean energy technologies including, electric vehicles and wind turbines. Currently, REE are predominantly produced from carbonatite ores and ion adsorption clay deposits (Dushyantha et al., 2020) but forecasts have suggested that these deposits may not be able to meet future demand, leading to potential shortages (Gielen and Lyons, 2022). Additionally, increased mining of REE from primary sources will result in significant environmental and ecological impacts including REE contamination (Golroudbary et al., 2022). Consequently, increased attention is being given to low-temperature and sedimentary environments as secondary sources of REE such as: (i) acid mine drainage (AMD) and mine tailings (Royer-Lavallée et al., 2020; León et al., 2021a); (ii) coal and coal fly ash (Seredin and Dai, 2012; Blissett et al., 2014); (iii) oil sand tailings (Roth et al., 2017); and (iv) formation waters including geothermal and petroleum brines (e.g. Quillinan et al., 2018; Smith et al., 2017). Recovery of REE from these sources promises to have lower environmental footprints and capital costs, while also enhancing the circular economy by using waste as the REE source (Dang et al., 2021). Moreover, their global distribution reduces domestic supply concerns (Pawar and Ewing, 2022) helping nations attain mineral security which is critical for achieving many of the United Nations' Sustainable Development Goals (SDGs) (Franks et al., 2022).

Exploration and recovery of REE from secondary sources are only in early stages. Therefore, determining the setting and mechanisms of REE transport and enrichment is crucial for exploration and the developing suitable extraction processes. A common factor among these sources is the association of REE with clay minerals and fine-grained sediments. For example, REE concentrations in formation waters of Saskatchewan were greatest in formations predominantly composed of fine-grained clastics relative to those with a high carbonate content (Bishop et al., in review). Similarly, analysis of a global dataset of REE in sedimentary lithologies indicated that REE are more enriched in fine-grained clastic rocks including shales and siltstones compared to carbonates, evaporites, and coarser grained clastic lithologies (Bishop and Robbins, in review). In coals, detrital and clay minerals are major REE-bearing phases that control their abundance in ashes (Dai et al., 2021; Fu et al., 2022). Additionally, the shales of the Iberian Pyrite Belt could be a significant source of REE to AMD waters (León et al., 2023) where their transport at neutral to basic pH conditions is dominated by particulate phases including clays (Olías et al., 2018). The importance of the relationship between REE and clay minerals is well established for secondary sources, but surprisingly, there is a dearth of information. regarding the binding behavior of REE to clay mineral surfaces. Clay minerals comprise a significant component of

particulate matter in rivers, are amongst the most important solid-phase carriers for trace elements (Viers et al., 2009), and they are the main constituent of most marine sediments (Machado et al., 2005). Moreover, given that clay minerals have high specific surface areas and surface functional group concentrations, and are ubiquitous in natural environments, the adsorption of REE to clay minerals may be an important control on REE transport and enrichment.

In aqueous environments, REE speciation and mobility are controlled by both the geochemical properties of the fluids and reactive particles and surfaces in the system, each of which have important implications for transport, enrichment, and recovery. REE are typically dissolved under acidic pH conditions, whereas at circumneutral and alkaline pH, adsorption and/or co-precipitation with Fe oxyhydroxide (Olías et al., 2018), Al hydroxide (Ayora et al., 2016), Mn oxide (Liu et al., 2018), or clay minerals (Machado et al., 2005) commonly control REE speciation. Geochemical modelling techniques, such as surface complexation modelling (SCM) can be used to calculate and predict the speciation and adsorption of ions in the presence of charged ligands (Fein et al., 1997; Fowle and Fein, 1999). More recently, SCMs have been developed to predict REE adsorption to environmental media including bacteria (Ngwenya et al., 2009; Martinez et al., 2014), amorphous iron-oxyhydroxides (i.e. hydrous ferric oxide HFO ; Liu et al., 2018), amorphous hydrous manganese oxides (HMO; Pourret and Davranche, 2013), basaluminite (Lozano et al., 2019a), and schwertmannite (Lozano et al., 2020). Previously developed SCMs for REE binding to clay minerals considered the adsorption of Eu, however it behaves differently than other REE due to its reduction from Eu^{3+} to Eu^{2+} in under certain conditions (Bradbury and Baeyens, 2002, 2005, 2009; Bradbury et al., 2005). Additionally, it is important to determine whether adsorption complexes exist as inner- or outer-sphere, since ions bound as outer-sphere complexes are more easily leachable through ion exchange reactions (Mukai et al., 2020).

In this study, the adsorption of praseodymium (Pr), dysprosium (Dy), and ytterbium (Yb), representing a range of light to heavy REE, to two clay minerals (illite and kaolinite) was probed through SCM coupled with extended X-ray absorption fine structure (EXAFS). Thermodynamic stability constants for each REE-clay system were derived from pH edge adsorption experiments and utilized in predictive geochemical modelling to assess the ability of clay minerals to adsorb REE in competitive multi-sorbent systems. Finally, EXAFS curve fitting was performed to constrain the coordination environment of the adsorbed REE to each clay mineral. Our work is solely focused on the role of clay minerals in the transport and deposition in aqueous and sedimentary environments, as ion adsorption clay deposits are well characterized (Sanematsu and Watanabe, 2016). The work advances the understanding of REE adsorption to clay minerals which can aid in the identification potential secondary sources and development of effective recovery strategies.

Materials and Methods

Clay Preparation and Adsorption Experiments

Samples of kaolinite (KGa-2) and illite (IMt-2) were obtained from the Clay Mineral Society, Source Clays Repository (Purdue University, Indiana, USA) and were prepared based on the methods described in Hao et al. (2018). Clay mineral samples were pulverized using a mortar and pestle, then passed through a 100-mesh (0.149 mm) sieve. To homogenize the surface and

interlayer ions, the clays were subjected to three washes in a 0.1 M sodium nitrate solution (ACS certified, Fisher Scientific). Each wash cycle was allowed to equilibrate for 3 h followed by centrifugation at 10,000 g for 2 min, with fresh solution used for each wash cycle. Finally, the clays were frozen at -20°C for 12 h and subsequently freeze dried.

Adsorption experiments followed methods similar to Bishop et al. (2019). Stock solutions of Pr, Dy, and Yb were prepared by diluting 1000 part per million (ppm) certified standards (NIST SRM; Spex Certiprep) to 1 ppm of the REE of interest in 18.2 MΩ·cm water with either 0.01 M or 0.56 M NaCl (Fisher Scientific). Clay minerals (kaolinite or illite) were suspended in the REE solution to obtain a 1 g L^{-1} mixture and 10 mL volumes were partitioned into 50 mL polypropylene centrifuge tubes and pH adjusted to cover a range of 3 to 9 using small aliquots of 0.1 M NaOH or HCl (Trace metal grade, Fisher Scientific), as required. Samples were then rotated at 40 rpm for 24 hours. The equilibration time was sufficient to achieve equilibrium for REE adsorption to clay particles (Coppin et al., 2002). All glass and plasticware were acid-washed in 10% v/v HCl for a period of 24 hours followed by rinsing three times with 18.2 MΩ·cm ultra-pure water before use.

Following the equilibration period, the final pH of each sample was measured then filtered through a 0.2 µm nylon membrane and diluted 1:10 in 2% HNO_3 (Trace metal grade, Fisher Scientific). The concentration of REE in each solution was determined by Inductively Coupled Plasma Mass Spectrometry (ICP-MS/MS; Agilent 8800 Triple Quadrupole, Environmental Geochemistry Laboratory, University of Alberta) in no gas mode with a 2 ppm Lu internal standard, calibrated by a series of 11 external standards covering a range of 30 parts per trillion (ppt) to 1 ppm, using commercially available ICP-MS standards (NIST SRM; Spex Certiprep). Following analysis, the adsorbed fraction was calculated based on Equation 1:

$$Adsorbed\ fraction = \frac{[REE]_{initial} - [REE]_{final}}{[REE]_{initial}} \quad (1)$$

where $[REE]_{initial}$ is the measured concentration of the solution prior to the addition of clay particles, and $[REE]_{final}$ is the measured concentration of the solution following adsorption.

XAS Analysis and Data Processing

The speciation and coordination environment of yttrium (Y), used as a proxy for the lanthanides, was investigated by synchrotron based XAS at the Hard X-Ray Microanalysis (HXMA) beamline of the Canadian Light Source (CLS: Saskatoon, Saskatchewan, Canada). The Y K-edge (17038 eV) was probed since the K-edge of the Pr, Dy, and Yb is outside the energy range of the beamline, their respective L-edge energies are less sensitive and susceptible to interferences from more abundant elements, and there is a larger amount of crystallographic data available for modelling Y XAS data. XAS experiments were performed in a manner similar to Alam et al. (2020) using a double Si (111) crystal monochromator detuned to 40% to reduce the influence of higher-order harmonics with data collected in fluorescence mode by a 16-element solid state Ge detector. REE-loaded clay samples were prepared following the pH edge experiments at pH 6.5 and an ionic strength of 0.01 M, representing circumneutral conditions where >95% of the Y would be adsorbed to the clay. Following the 24 h equilibration period, samples were centrifuged to form wet pellets and secured to sample holders using Kapton tape oriented 45° to the incident beam. The energy steps for the scans were 10 eV with a 1s dwell time

in the pre-edge region, 0.5 eV with a 1s dwell time in the XANES region, and 0.05k with a 3s dwell time in the EXAFS region. A minimum of three scans were performed for each sample to improve the signal to noise ratio. The XAS data was processed using the ATHENA software (Ravel and Newville, 2005) for energy alignment and background subtraction. Based on the selected structural models, ATOM software (Ravel, 2001) was used to generate a FEFF7 input code. The theoretical EXAFS scattering amplitudes were then calculated using FEFF7.02 (Rehr and Albers, 2000) and EXAFS curve fitting was performed using WinXAS (Ressler, 1997).

Results and Discussion

Rare Earth Element Adsorption to Clay

REE adsorption was influenced by pH, ionic strength, and clay mineralogy (Figure 1A-F). pH played the greatest role in REE adsorption, with a stronger impact on adsorption for kaolinite than illite. A lower degree of REE adsorption was observed under acidic pH values but it progressively increased as a function of rising pH, with >95% adsorption achieved at approximately pH 7. This trend has been attributed to an increasingly negative surface charge of the sorbent due to progressive deprotonation of surface sites which provides a locus for cation adsorption as pH rises (Konhauser et al., 2020). The trend has been observed for a range of environmental surfaces, including: bacteria (Fein et al., 2001), clay minerals (Bachmaf and Merkel, 2011), biochar (Alam et al., 2018), and ferrihydrite (Dzombak and Morel, 1990; Tian et al., 2017) and for REE adsorption to schwertmannite (Lozano et al., 2020), basaluminite (Lozano et al., 2019a), *Bacillus subtilis* (Martinez et al., 2014), HFO (Liu et al., 2017), and HMO (De Carlo et al., 1997; Liu et al., 2018).

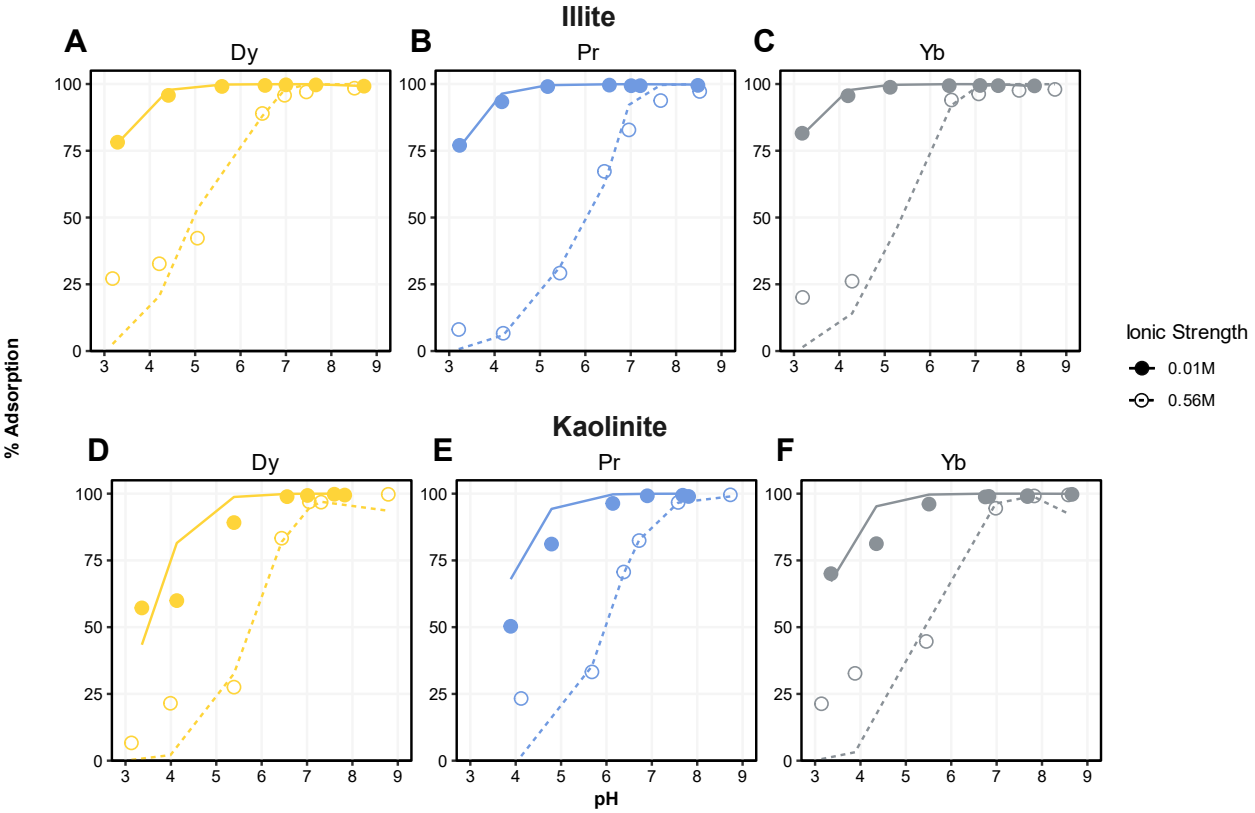

Figure 1 – pH edges for each REE-clay system (A-C: illite; D-F: kaolinite) displaying the percent REE adsorption as a function of pH at 0.01 M (solid line, closed circle) and 0.56 M (dotted line, open circle) ionic strengths. Circles represent the experimental data while the lines represent the best fit FITEQL model.

Ionic strength affected REE adsorption, with higher ionic strengths resulting in decreased REE adsorption to the clay minerals. At pH 3, the 0.56 M ionic strength experiments had approximately 50% less adsorption of each REE for illite and 40% less for kaolinite compared to the 0.01 M ionic strength experiments. The effect of ionic strength diminished once the pH increased above 7, where adsorption was greater than 95% in all systems. Hao et al. (2019) attributed the decrease in proton adsorption to clay minerals as ionic strength increased to a decrease in the clay particle's electrostatic field. However, Coppin et al. (2002) and Alessi and Fein (2010) postulated that at high ionic strength, site occupancy by monovalent cations hinders the adsorption of divalent and trivalent ions.

Illite had a higher REE adsorption affinity than kaolinite at both ionic strength conditions considered, similar to a trend observed by Hao et al. (2020) for Cd adsorption. The adsorption affinity of each clay studied is largely driven by their structural configuration, with illite being composed of two tetrahedral sheets fused to an octahedral sheet, while kaolinite only contains one tetrahedral sheet, resulting in a higher concentration of surface functional sites and cation exchange capacity for illite (Sposito et al., 1999).

Surface Complexation Modelling

A SCM is composed of a system of balanced reactions for which there are corresponding mass action (K) constants for the formation of aqueous and surface complexes and the precipitation of solid phases (Fein, 2006; Flynn et al., 2014). Surface complexation modelling has been developed and widely applied to study both the protonation of reactive surface sites on bacterial cell walls and mineral surfaces (e.g. Schad et al., 2019; Warchola et al., 2017) and the adsorption of various ions (Boyanov et al., 2003; Borrok and Fein, 2005) and have been used to predict metal adsorption in multi-component systems (Bishop et al., 2019). Despite their difficulty to develop, they have more applicability than empirical adsorption models because they can account for changing environmental conditions including pH, ionic strength, the presence of competing species, the sorbent to sorbate ratio, and changes in the aqueous speciation of a metal (Alessi et al., 2019).

The thermodynamic binding constants for each REE-clay systems were calculated from the results of the pH edge adsorption experiments using least-squares optimization implemented in FITEQL v4.0 (Herbelin and Westall, 1999). Site concentrations and pKa values for both clay minerals in 0.01 M ionic strength solutions were previously reported (Hao et al., 2019) (Table 1). Hao et al. (2019) derived a linear relationship between K values and ionic strength and based on these values, the K values for 0.56 M ionic strength was calculated (Hao et al., 2020). Hao et al. (2019, 2020) invoked a two-site model to describe proton adsorption to each clay, involving an amphoteric surface functional group (≡XOH) and a permanently charged structural functional group (≡XLH). The binding of each REE to the clay surface sites is given as:

$$\equiv XOH + REE^{3+} \leftrightarrow XOREE^{2+} + H^{+} \quad (2)$$

$$\equiv XLH + REE^{3+} \leftrightarrow XLREE^{2+} + H^{+} \quad (3)$$

Accordingly, the mass action equations for the adsorption reactions are given in Equations 4 and 5:

$$K_{XOREE} = \frac{[\equiv XOREE^{2+}] \cdot \alpha_{H^+}}{[\equiv XOH] \cdot \alpha_{REE^{3+}}} \quad (4)$$

$$K_{XLREE} = \frac{[\equiv XLREE^{2+}] \cdot \alpha_{H^+}}{[\equiv XLH] \cdot \alpha_{REE^{3+}}} \quad (5)$$

where K_{XOREE} and K_{LREE} are the stability constants for each adsorption reaction, and α is the activity of the aqueous species.

Clay	Ionic Strength (mol/L)	XLH pKa	XLH Site Concentration (mol/L)	XO-	XOH	XOH Site Concentration (mol/L)	Total Site Concentration (mol/L)
Illite	0.01	-5.917	5.53E-05	-10.119	9.734	8.48E-05	1.40E-04
Illite	0.56	-5.236	4.56E-05	-10.216	9.407	7.83E-05	1.24E-04
Kaolinite	0.01	-10.026	1.02E-04	-7.274	5.346	2.32E-05	1.25E-04

Kaolinite	0.56	-9.21	1.96E-05	-6.01	4.492	1.84E-05	3.80E-05

Table 1 - Modelling parameters including the pKa site concentration values for the kaolinite and illite structural (XLH) and amphoteric (XOH) sites used in the development of the SCM derived from (Hao et al., 2019, 2020).

Aqueous complexation of REE by anions was considered by using previously determined hydrolysis (Klungness and Byrne, 2000) and chloride (Luo and Byrne, 2001) stability constants (Table S1). Carbonate complexation was not incorporated as the adsorption of REE to clays does not depend on the presence of aqueous inorganic carbon species (Coppin et al., 2002).

The derived thermodynamic mass action constants determined by the FITEQL modelling for each clay at both ionic strength conditions are shown in Table 2. A non-electrostatic model (NEM) provided a good fit for the data in each system. This approach is consistent with previous studies that have found that NEMs sufficiently explain REE adsorption to charged surfaces (Bradbury and Baeyens, 2002; Lozano et al., 2019a). The models fit the data well for illite across the entire experimental pH range. However, kaolinite adsorption was overpredicted between pH 3.5 and 5, and underpredicted below pH 3.5 for Pr and Yb. The model also under-predicted REE adsorption at acidic pH values for the 0.56 M ionic strength experiments. Adsorption to both the structural (XLH) and amphoteric (XOH) groups provided a suitable fit for REE adsorption to illite at each ionic strength, with the exception of Pr adsorption at 0.01 M ionic strength, which only invoked adsorption to the XLH site. REE adsorption to kaolinite was best modelled by invoking adsorption only to the XLH site.

Clay	Ionic Strength (M)	Site	Dy	Pr	Yb
Illite	0.01	XLH	1.562	1.586	1.752
		XOH	0.289	N/A	0.253
Kaolinite		XLH	0.533	0.455	0.976
Illite	0.56	XLH	-0.413	-0.743	-0.377
		XOH	1.593	0.951	1.917
Kaolinite		XLH	-0.589	-0.906	-0.358

Table 2 - Log K values for each clay-REE system calculated by FITEQL modelling for 0.01 M and 0.56 M ionic strengths.

The mass action constants for Pr, Dy, and Yb adsorption are similar to those reported for Eu adsorption onto the structural site of illite (1.9) (Bradbury and Baeyens, 2009). The utility of these binding constants is in predicting the speciation and binding affinity of REE in the presence of competing charged surfaces and under changing solution conditions and are applied to assess the relative affinities of clay minerals in a competitive setting in the section "Predictive Geochemical Modelling".

Synchrotron XAS

The Fourier transformed (FT) EXAFS spectra were similar for both illite and kaolinite with a peak at 1.9 Å, attributed to the first O shell, and a second peak at ~2.9 Å, which corresponded to outer shell Y-Si coordination (Figure 2). The EXAFS fits for the first shell invoked Y-O bonding

at 2.24 to 2.39 Å with an overall coordination number of 11.5 for illite and 10.2 for kaolinite (Table 3), larger than the aqueous Y coordination of 8 which had a similar Y-O bond distance of 2.35 Å (Díaz-Moreno et al., 2000). This is indicative of outer-sphere complexation since the Y retains a full hydration sphere and is bound to the clay surface by electrostatic forces between water molecules and oxygens on the surface of the clay mineral (Borst et al., 2020). Conversely, the second shell displays Y-Y and Y-Si bonding with notably smaller coordination numbers which can be attributed to the hydrolysis of edge and basal hydroxyl groups in the clay structure with increasing pH and is indicative of inner-sphere complexation (Stumpf et al., 2002, 2007). These results indicate the Y can participate in both inner- and outer-sphere complexation with the clay surface.

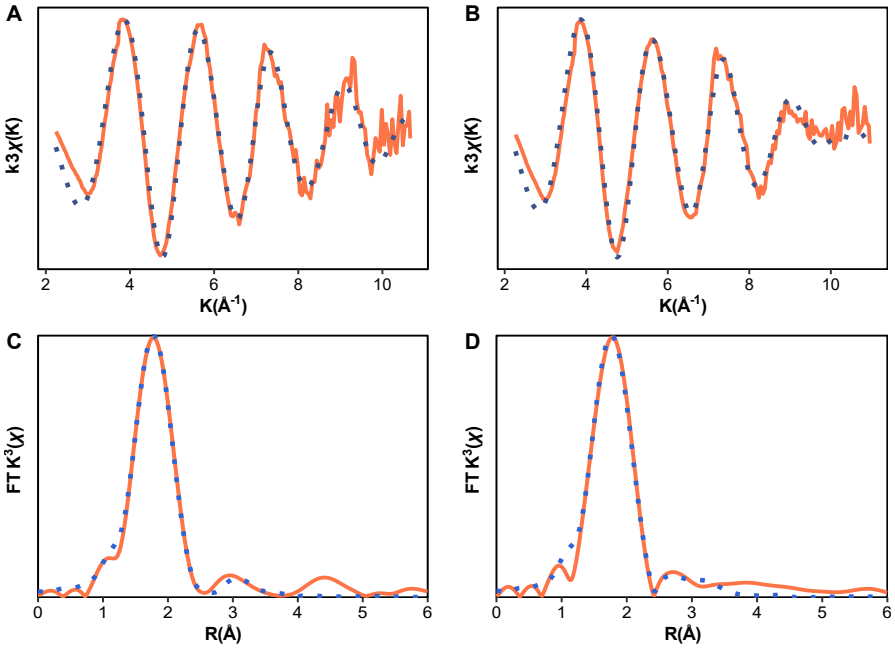

Figure 2 - k^3 weighted EXAFS results of the Y K-edge for adsorption to illite (A) and kaolinite (B). Corresponding phase-shifted Fourier transformed EXAFS data for illite (C) and kaolinite (D). Orange lines represent the experimental data and the dotted blue lines display the EXAFS curve fits.

Clay	Shell	Path	CN (±0.5)	R (±0.02Å)	DW (15-20%)
Illite	1st	Y-O	5.3	2.25	0.0022
		Y-O	6.2	2.39	0.0019
	2nd	Y-Y	0.6	3.55	0.0095
		Y-Si	2.8	3.03	0.0070
Kaolinite	1st	Y-O	4.7	2.24	0.0022
		Y-O	5.5	2.39	0.0019
	2nd	Y-Y	0.5	3.55	0.0095
		Y-Si	2.3	3.01	0.0070

Table 3 - EXAFS fit results for Y adsorption to illite and kaolinite. CN: coordination number. R: radial distance. DW: Debye-Waller Factor.

This is supported by previous works which demonstrated that Y adsorption to clay minerals can form both inner- and outer-sphere complexes. Stumpf et al. (2002) determined that Eu can form both types of complexes with kaolinite and illite clays using time-resolved laser fluorescence spectroscopy (TRLFS) and Finck et al. (2017) showed that Y formed inner-sphere complexes with hectorite by way of EXAFS. In terms of natural ion-adsorption clays, Mukai et al. (2020) suggested that the adsorption of REE to kaolinite forms inner-sphere complexes based on findings from electron microscopy. In contrast with our work which identified second shell Y-Si inner-sphere complexation, EXAFS analysis by Borst et al., (2020) indicated Y retains a full hydration sphere when adsorbed to kaolinite and present as an outer-sphere complex. Additionally, the absence of Y-Al and Y-Si suggested a lack of inner-sphere complexation. Inner-sphere REE complexes have been found for other media including bacteria (*Pantoea agglomerans)* (Ngwenya et al., 2009), basaluminite from an AMD-affected environment (Lozano et al., 2019b), and Fe and Mn oxyhydroxides (Ohta et al., 2009).

At higher pH and ionic strength, desolvation of REE ions can lead to inner-sphere complexes forming on either aluminol (Al-OH) or siloxane (Si-O-Si) surfaces or terminal OH ligands (Borst et al., 2020). Coppin et al. (2002) suggested that at higher ionic strength, REE adsorption takes place on amphoteric sites, leading to the formation of inner-sphere complexes to compensate for the variable charge, whereas at lower ionic strength, adsorption may form outer-sphere complexes. Additionally, Stumpf et al. (2002) indicated that inner-sphere Eu complexation can begin at lower pH values at higher ionic strength. Here, both types of complexes were found to form under low ionic strength conditions, where they are likely being bound to both the clay interlayers and surface.

The coordination environment has important implications for designing extraction processes. It has been shown that ions bound as outer-sphere complexes are more easily leachable than inner-sphere complexes and can be recovered through relatively simple ion-exchange processes (Mukai et al., 2020). However, the results here indicate that an additional step may be required to recover the more tightly bound, inner-sphere complexed REE.

Predictive Geochemical Modelling

Predictive geochemical modelling was undertaken to assess the relative REE binding affinities for environmental media which included humic acid, *B. subtilis*, HMO, HFO, and clay minerals. These phases were selected as representative of common surfaces or organic acids in aqueous environments whose ability to adsorb REE has been previously studied. Aqueous speciation was calculated using the SpecE8 code in Geochemist's Workbench (Community Edition, Version 15) utilizing the Thermoddem_V1.0.3.4 database which includes REE-carbonate, -hydrolysis, and -chloride complexes (Blanc et al., 2012). The database was modified to include protonation and REE binding constants for kaolinite and illite from this study, HFO (Liu et al., 2017), HMO (Tonkin et al., 2004; Pourret and Davranche, 2013), *Bacillus subtilis* (Fein et al., 1997; Martinez et al., 2014), and humic acid (Pourret et al., 2007). Only the humic acid binding constant for the "A" site was considered as the "B" site is not well constrained. Full model

parameters are summarized in Table S1. The relative REE adsorption affinity of each sorbent was modelled using two different scenarios: (1) equivalent site concentrations (5 x 10^{-5} mol/L) and (2) equivalent masses of each sorbent (0.25 g/L) using realistic site proportions. Each model was run at 25°C in a 0.01 M NaCl solution, and across a pH range of 3 to 9. The solution was in equilibrium with atmospheric CO_2 and at an initial total metal concentration of 1 ppm (either Pr, Dy, or Yb). For clay minerals, the binding constants for the 0.01 M ionic strength experiments were utilized.

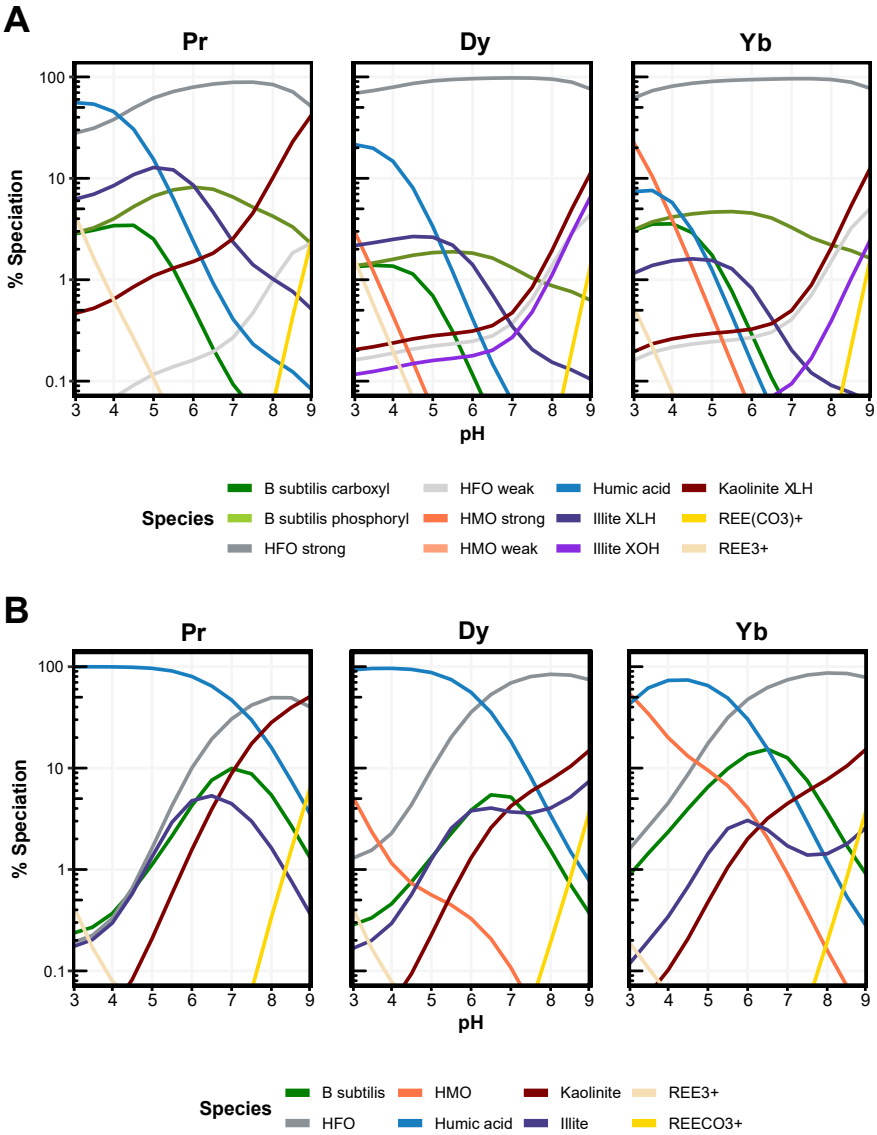

Figure 3 – Results of the predictive geochemical modelling to identify the dominant REE species across a pH range of 3 to 9. A – modelling with an equivalent number of sites (5x10^{-5} mol/L) for each ligand. B – modelling with an equivalent mass (0.25 g/L) of each sorbent.

The first scenario (Figure 3A) determined the relative REE binding affinity to common environmental surface functional groups, assuming the same number of proton-active sites for each functional group. The resulting predictions showed that in these mixed sorbent systems, the

HFO strong site dominated REE speciation across the entire pH range for each REE, while adsorption to the humic acid "A" site was also important at acidic pH values. At circumneutral pH, the binding affinity of the *B. subtilis* phosphoryl site and the illite structural site increased, while the *B. subtilis* carboxyl site, HMO strong site, humic acid "A" site, and aqueous REE ions decreased. Above pH 7, kaolinite, illite amphoteric sites (with the exception of Pr), HFO weak site, and REE carbonate became increasingly important.

The second scenario (Figure 3B) examined the adsorption of REE on a mass normalized basis, assuming that the mixed system included 0.25 g/L of each sorbent and accounted for the proportions of each sorbents' functional group types. At low pH values, HMO and humic acid dominated Dy and Yb speciation, while Pr speciation was dominated by only humic acid (>99%). At circumneutral pH, HFO, humic acid, illite, kaolinite, and *B. subtilis* each play a role in Pr speciation, while humic acid and kaolinite controlled Dy speciation while *B. subtilis* was also important for Yb speciation. HFO and montmorillonite had the highest Yb adsorption at circumneutral pH. Finally, at pH values >8, HFO, and kaolinite adsorbed the majority of REE in solution. Although illite and kaolinite had among the lowest site concentrations per gram among the sorbents considered, they still played a role in REE speciation. The strong complexation by humic acid at low pH could be attributed to it having the highest concentration of sites per gram. The modelling also underscored the strong affinity of the HFO strong site to adsorb REE. In the equivalent mass comparison modelling (Scenario 2) at circumneutral pH, it had among the highest REE adsorption despite having approximately 10x fewer sites than the other sorbents.

The predictive models highlighted the impact of clay minerals on REE speciation, especially when the pH is greater than 7, and therefore they should be considered in geochemical models focusing on REE transport. In aqueous environments, REE speciation is a result of the relative stability of REE complexes and REE are typically associated with particulate matter under circumneutral pH conditions (Alibo and Nozaki, 1999; Verplanck et al., 2004). However, these models often downplay the importance of clay minerals, since the other sorbents may not be found in as high abundance in natural systems or be stable across the entire pH range examined. For example, Fe hydroxysulfate minerals, such as schwertmannite, a common mineral in AMD, are only stable from pH 2-4, while ferrihydrite does not precipitate until the pH is above 5 (Sánchez España, 2007). Similarly, humic acids have also been shown to form insoluble aggregates under acidic pH conditions (Lan et al., 2022) and many common bacteria cannot survive strongly acidic or basic conditions. Since clays are stable across a wide pH range, competition among other sorbents could be reduced, especially in more extreme environments such as AMD, at high salinity, or at low temperatures where kinetics could control the precipitation of mineral phases. Under these conditions, clays could control REE speciation, especially since the EXAFS modelling indicated they can form inner-sphere complexes which are more difficult to leach and would not be out-competed by other sorbents, thereby carrying the REE from source to sink. However, this modelling only considered adsorption, and does not take into account precipitation, aggregation, or the presence of other species important for REE transport such as basaluminite or schwertmannite which are common in AMD. Similarly, colloids could play a role in aqueous REE

transport. For instance, Munemoto et al. (2014) found that colloids >2 µm controlled REE mobility in groundwater, while von Gunten et al. (2019) found that the majority of trace metals in meromictic mine pit lakes were associated with colloids (<10 kDa).

Role of Clays in Alternative Sources of REE

The anticipated increase in global REE demand due to their role in the energy transition has led to significant interest in extracting REE from new, secondary sources including AMD, formation and geothermal waters, coal waste, and oilsands tailings. A common factor among these sources is the role of clay minerals. AMD has received attention as a source of REE because, due its low pH, it can contain metal concentrations up to four orders of magnitude higher than unpolluted waters (Gimeno Serrano et al., 2000; Stewart et al., 2017). Estimates for the total value of the REE flux in AMD ranges from $5.4 million in the Iberian Pyrite Belt, (León et al., 2021b) up to $303 million from the Appalachian Basin (Vass et al., 2019b). REE speciation in AMD is controlled by pH, where they predominantly occur as a mixture of free ions and sulphate complexes at low pH (Gimeno Serrano et al., 2000; Verplanck et al., 2004). However, their concentration decreases with increasing pH due to adsorption to particulate matter and co-precipitation with Al and/or Fe at circumneutral to alkaline pH values (Olías et al., 2018; Vass et al., 2019b). Clay minerals, specifically illite and kaolinite, comprise an appreciable component of the sediment in the Huelva estuary of the Tinto and Odiel rivers (Galán et al., 2003) and are an important control on REE transport (Cuadros et al., 2023). Moreover, normalized REE patterns between the waters and rocks in the Iberian Pyrite Belt demonstrate a geochemical relationship between AMD and shales (León et al., 2023).

Groundwater and basinal brines produced as a by-product of geothermal energy production or hydrocarbon extraction have also been touted as possible REE sources. Although these waters have received less attention than AMD, the mechanisms controlling REE concentrations are similar, being strongly dependent on pH, ionic strength, and the presence of competing anions and cations in addition to fluid temperature (Lewis et al., 1998). Noack et al. (2014) found that REE concentrations were higher at lower pH values, with scavenging by clays, oxides, and/or co-precipitation occurring at neutral and basic pH. In geothermal waters from western Yunnan, China, REE concentrations showed a negative correlation with the total dissolved solids (TDS), while the TDS has a positive correlation with temperature (Zhang et al., 2016). This was attributed to REE in waters with elevated temperature and TDS being adsorbed and incorporated into clay-bearing sediments. This inverse relationship with TDS was also observed by Bishop et al. (in review) in basinal brines of Saskatchewan, where the highest REE concentrations were in waters with among the lowest TDS. Additionally, lithology and the geologic history of the basin can also be significant factors; Bishop et al. (in review) found that REE concentrations were higher in brines hosted in clastic dominated formations with the highest concentrations in formations with a higher fine-grained component. The higher REE concentrations in brines also corresponded with shales and mudstones having the highest REE concentrations in the Western Canada Sedimentary Basin (Bishop and Robbins, in review). This relationship could indicate water-rock interactions with fine-grained materials being the main source of REE in the brines, which is supported by leaching experiments from rocks of the Iberian Pyrite Belt where REE normalization patterns were

transferred from rocks into solution, indicating water-rock interactions as an important source of REE to the waters (León et al., 2023). However, determining the source of REE could be considerably more complicated. Quillinan et al. (2018) observed that while lithology is important, basinal controls and geologic history also play an important role in determining brine REE concentrations. For the transport and accumulation of REE in marine sediments, REE are typically transported in bulk from source to sink (Condie, 1991) and clay minerals are the dominant source of REE to the oceans (Abbott et al., 2019), implying that a source with elevated REE concentrations could translate to shales and subsequently brines with high REE abundances.

Additional secondary sources from the energy industry have been studied, including oilsands tailings, coal, and coal waste. The highest concentrations of REE in oilsands tailings from Alberta occur in the fine fraction that has a high kaolinite component (Roth et al., 2017). Similarly, coal and coal waste can also have elevated REE concentrations (Seredin et al., 2013; Blissett et al., 2014). They have been studied extensively in recent years and are the most promising of the examples investigated in this study. The most common REE-bearing phases in coals include detrital, authigenic, and clay minerals (Fu et al., 2022). The REE host in coals can vary, and in bituminous coals, Finkelman et al. (2018) found REE were primarily associated with phosphate minerals, whereas in lower rank coals, the majority of REE are found with clay minerals. Similarly, REE in a Pennsylvanian anthracite were also associated with clay minerals (Hower and Dai, 2016). Analysis of the USGS CoalQual Database has shown a correlation between the total REE and Al contents in coal, suggestive of REE partitioning into coal by clay or other detrital components (Feng et al., 2020). Sequential leaching experiments of anthracite from the Qinshui Basin, China indicated that REE were mainly bound to clay minerals and residual organics (Wang et al., 2019). Geochemical and statistical analysis of a compiled global coal ash dataset indicates that REE in coal ashes are linked to elements typically associated with detrital and clay minerals, including Al, Ti, Th, and Zr, indicating clays may be the main source of REE in many coal deposits (Bishop et al., 2023). Some of the highest concentrations of REE in coal deposits globally, such as the Fire Clay coals of the Appalachian Basin, are related to tonsteins: clay rich volcanic layers (Hower et al., 2015). Therefore, identifying coal ashes sourced from deposits with an elevated clay content may be the first step in an exploration process to find the most suitable ashes for REE recovery.

In each of these secondary sources, clay minerals play a crucial role in REE enrichment. Better understanding the impact of clay minerals in each of these secondary sources has implications when examining their REE potential, since transport and deposition of REE can be predicted by incorporating clays into a mineral "system" and including these derived stability constants. Additionally, the binding of REE to clays is also crucial to consider when designing recovery processes since REE bound to clay minerals are typically leached by cation exchange with monovalent inorganic salts and transferred into solution as soluble sulfate or chloride complexes (Moldoveanu and Papangelakis, 2012). The REE can then be recovered as high purity end-product via solvent extraction, ion-exchange, or selective precipitation with oxalic acid to produce oxalates which are subsequently converted to rare earth oxides via roasting (Moldoveanu and Papangelakis, 2012). Similarly, there has been significant research into different processes to

recover REE from coal ash which are significantly more efficient and environmentally friendly than mining REE from ore deposits (e.g. Stoy et al., 2021; Liu et al., 2023; Dardona et al., 2023).

Environmental Implications

Currently, China dominates the global REE supply chain including production and processing, which has sparked supply concerns and resulted in their classification as "Critical Minerals" by several countries who are looking to solidify their own supply chains (Natural Resources Canada, 2022; USGS, 2023). The current imbalance poses a significant challenge to advancing sustainable technologies, especially as demand is anticipated to significantly increase due to the propagation of REE in sustainable energy technologies required to reduce the impacts of climate change, such as wind turbines and electric vehicles (Pawar and Ewing, 2022). The growth of REE mining is complicated by significant chemical use, energy requirements, and environmental impacts such as land and water use, radioactive tailings, human health, and social issues. For instance, the extraction of 1 tonne (t) of REE at Bayan Obo requires 4.41 t of sulphuric acid, 12.32 t of sodium chloride, 1.64 t of sodium hydroxide, 1.17 t of hydrochloric acid, and 1.90 t of water and requires 38 to 48 GJ of energy (Yin et al., 2021). Increased mining has also raised concerns about REE themselves as contaminants in the environment since they can affect plants and animals as well as human organs (Yin et al., 2021). Accordingly, a better understanding of the fate and transport of REE in the environment is fundamental to ensure proper steps are taken to reduce these concerns. Sourcing REE from secondary sources can drastically reduce the material requirements and environmental impacts compared to mining ore deposits (Gaustad et al., 2021). The recovery of REE from sources such as AMD waters, formation and geothermal waters, and coal waste can convert a waste stream into an asset, reducing ecological and social impacts (Vass et al., 2019a; Hedin et al., 2020). Additionally, their recovery can be part of a remediation strategy (Pan et al., 2019; León et al., 2021b; Miranda et al., 2022). Mining waste is a significant problem for many coal and metal sulfide deposits but the ability to valorize the waste presents an opportunity to extract new metals of economic interest while reducing the impacts of legacy tailings (León et al., 2021a). Drainage from inactive and abandoned coal mines is also a significant environmental issue, and precipitates formed through AMD treatment can be processed for REE (Stewart et al., 2017). Similarly, there are significant concerns about the long term storage of coal ash which can have catastrophic environmental impacts, such as the Kingston Ash Spill in Tennessee (Rivera et al., 2015). Assessing the economic potential of each of these secondary sources require a greater understanding of the transport and enrichment processes by which they formed. Due to the importance of clay minerals in each of these sources, it is crucial to better constrain the interplay between clay minerals and REE. This study contributes to the growing knowledge of REE complexation in the environment and the thermodynamic binding constants can be applied to better determine the transport and fate of REE which may then be used to assist in discovering and developing new sources of REE. The insights from the EXAFS are important for identifying whether REE are readily released from the clays under varying conditions which has implications for the source and for designing extraction processes. Ultimately, economic considerations and the creation of an efficient, cost-effective recovery strategy will dictate whether any of these settings can become a secondary source of REE, which can alleviate supply chain concerns and provide the raw materials necessary for the energy transition.

Conclusions depending on journal. Basically just summarize everything and take half of the last section.

Acknowledgements

The authors would like to acknowledge the financial contributions of the Natural Sciences and Engineering Research Council of Canada (NSERC) in the form of a Canada Graduate Scholarship – Doctoral (CGS-D: BAB) and Discovery Grants (LJR: RGPIN-2021-02523, KOK: RGPIN-165831, and DSA: RGPIN-2020-05289) and the Canadian Light Source Inc. for Graduate Student Travel Grants to conduct analyses at the CLS (BAB, KRS).

References

Abbott A. N., Löhr S. and Trethewy M. (2019) Are clay minerals the primary control on the oceanic rare earth element budget? *Frontiers in Marine Science* **6**, 1–19.

Alam Md. S., Bishop B., Chen N., Safari S., Warter V., Byrne J. M., Warchola T., Kappler A., Konhauser K. O. and Alessi D. S. (2020) Reusable magnetite nanoparticles–biochar composites for the efficient removal of chromate from water. *Sci Rep* **10**, 19007.

Alam Md. S., Swaren L., von Gunten K., Cossio M., Bishop B., Robbins L. J., Hou D., Flynn S. L., Ok Y. S., Konhauser K. O. and Alessi D. S. (2018) Application of surface complexation modeling to trace metals uptake by biochar-amended agricultural soils. *Applied Geochemistry* **88**, 103–112.

Alessi D. S. and Fein J. B. (2010) Cadmium adsorption to mixtures of soil components: Testing the component additivity approach. *Chemical Geology* **270**, 186–195.

Alessi D. S., Flynn S. L., Alam S., Robbins L. J. and Konhauser K. O. (2019) Potentiometric Titrations to Characterize the Reactivity of Geomicrobial Surfaces. In *Analytical Geomicrobiology* (eds. J. P. L. Kenney, H. Veeramani, and D. S. Alessi). Cambridge University Press. pp. 79–92.

Alibo D. S. and Nozaki Y. (1999) Rare earth elements in seawater: particle association, shale-normalization, and Ce oxidation. *Geochimica et Cosmochimica Acta* **63**, 363–372.

Ayora C., Macías F., Torres E., Lozano A., Carrero S., Nieto J. M., Pérez-López R., Fernández-Martínez A. and Castillo-Michel H. (2016) Recovery of Rare Earth Elements and Yttrium from Passive-Remediation Systems of Acid Mine Drainage. *Environmental Science and Technology* **50**, 8255–8262.

Bachmaf S. and Merkel B. J. (2011) Sorption of uranium(VI) at the clay mineral-water interface. *Environmental Earth Sciences* **63**, 925–934.

Bishop B. A., Flynn S. L., Warchola T. J., Alam M. S., Robbins L. J., Liu Y., Owttrim G. W., Alessi D. S. and Konhauser K. O. (2019) Adsorption of biologically critical trace elements to the marine cyanobacterium Synechococcus sp. PCC 7002: Implications for marine trace metal cycling. *Chemical Geology* **525**, 28–36.

Bishop B. A., Shivakumar K. R., Alessi D. S. and Robbins L. J. (2023) Insights into the rare earth element potential of coal combustion by-products from western Canada. *Environ. Sci.: Adv.*, 10.1039.D2VA00310D.

Blanc Ph., Lassin A., Piantone P., Azaroual M., Jacquemet N., Fabbri A. and Gaucher E. C. (2012) Thermoddem: A geochemical database focused on low temperature water/rock interactions and waste materials. *Applied Geochemistry* **27**, 2107–2116.

Blissett R. S., Smalley N. and Rowson N. A. (2014) An investigation into six coal fly ashes from the United Kingdom and Poland to evaluate rare earth element content. *Fuel* **119**, 236–239.

Borrok D. M. and Fein J. B. (2005) The impact of ionic strength on the adsorption of protons, Pb, Cd, and Sr onto the surfaces of Gram negative bacteria: Testing non-electrostatic, diffuse, and triple-layer models. *Journal of Colloid and Interface Science* **286**, 110–126.

Borst A. M., Smith M. P., Finch A. A., Estrade G., Villanova-de-Benavent C., Nason P., Marquis E., Horsburgh N. J., Goodenough K. M., Xu C., Kynický J. and Geraki K. (2020) Adsorption of rare earth elements in regolith-hosted clay deposits. *Nature Communications* **11**, 1–15.

Boyanov M. I., Kelly S. D., Kemner K. M., Bunker B. A., Fein J. B. and Fowle D. A. (2003) Adsorption of cadmium to Bacillus subtilis bacterial cell walls: A pH-dependent X-ray absorption fine structure spectroscopy study. *Geochimica and Cosmochimica Acta* **67**, 3299–3311.

Bradbury M. H. and Baeyens B. (2005) Modelling the sorption of Mn(II), Co(II), Ni(II), Zn(II), Cd(II), Eu(III), Am(III), Sn(IV), Th(IV), Np(V) and U(VI) on montmorillonite: Linear free energy relationships and estimates of surface binding constants for some selected heavy metals and actinides. *Geochimica et Cosmochimica Acta* **69**, 875–892.

Bradbury M. H. and Baeyens B. (2009) Sorption modelling on illite Part I: Titration measurements and the sorption of Ni, Co, Eu and Sn. *Geochimica et Cosmochimica Acta* **73**, 990–1003.

Bradbury M. H. and Baeyens B. (2002) Sorption of Eu on Na- and Ca-montmorillonites: Experimental investigations and modelling with cation exchange and surface complexation. *Geochimica et Cosmochimica Acta* **66**, 2325–2334.

Bradbury M. H., Baeyens B., Geckeis H. and Rabung Th. (2005) Sorption of Eu(III)/Cm(III) on Ca-montmorillonite and Na-illite. Part 2: Surface complexation modelling. *Geochimica et Cosmochimica Acta* **69**, 5403–5412.

De Carlo E. H., Wen X. Y. and Irving M. (1997) The influence of redox reactions on the uptake of dissolved Ce by suspended Fe and Mn oxide particles. *Aquatic Geochemistry* **3**, 357–389.

Condie K. C. (1991) Another look at rare earth elements in shales. *Geochimica et Cosmochimica Acta* **55**, 2527–2531.

Coppin F., Berger G., Bauer A., Castet S. and Loubet M. (2002) Sorption of lanthanides on smectite and kaolinite. *Chemical Geology* **182**, 57–68.

Cuadros J., Mavris C. and Nieto J. M. (2023) Rare earth element signature modifications induced by differential acid alteration of rocks in the Iberian Pyrite Belt. *Chemical Geology* **619**, 121323.

Dai S., Finkelman R. B., French D., Hower J. C., Graham I. T. and Zhao F. (2021) Modes of occurrence of elements in coal: A critical evaluation. *Earth-Science Reviews* **222**, 103815.

Dang D. H., Thompson K. A., Ma L., Nguyen H. Q., Luu S. T., Duong M. T. N. and Kernaghan A. (2021) Toward the Circular Economy of Rare Earth Elements: A Review of Abundance, Extraction, Applications, and Environmental Impacts. *Arch Environ Contam Toxicol* **81**, 521–530.

Dardona M., Mohanty S. K., Allen M. J. and Dittrich T. M. (2023) From ash to oxides: Recovery of rare-earth elements as a step towards valorization of coal fly ash waste. *Separation and Purification Technology* **314**, 123532.

Díaz-Moreno S., Muñoz-Páez A. and Chaboy J. (2000) X-ray Absorption Spectroscopy (XAS) Study of the Hydration Structure of Yttrium(III) Cations in Liquid and Glassy States: Eight or Nine-Fold Coordination? *J. Phys. Chem. A* **104**, 1278–1286.

Dushyantha N., Batapola N., Ilankoon I. M. S. K., Rohitha S., Premasiri R., Abeysinghe B., Ratnayake N. and Dissanayake K. (2020) The story of rare earth elements (REEs): Occurrences, global distribution, genesis, geology, mineralogy and global production. *Ore Geology Reviews* **122**, 103521.

Dzombak D. A. and Morel F. M. M. (1990) *Surface Complexation Modeling: Hydrous Ferric Oxide*., John Wiley & Sons, Inc.

Fein J. B. (2006) Thermodynamic Modeling of Metal Adsorption onto Bacterial Cell Walls: Current Challenges. *Advances in Agronomy* **90**, 179–202.

Fein J. B., Daughney C. J., Yee N. and Davis T. A. (1997) A chemical equilibrium model for metal adsorption onto bacterial surfaces. *Geochimica et Cosmochimica Acta* **61**, 3319–3328.

Fein J. B., Martin A. M. and Wightman P. G. (2001) Metal adsorption onto baterial surfaces: Development of a predictive approach. *Geochimica et Cosmochimica Acta* **65**, 4267–4273.

Feng X., Onel O., Council-Troche M., Noble A., Yoon R.-H. and Morris J. R. (2020) A study of rare earth ion-adsorption clays: The speciation of rare earth elements on kaolinite at basic pH. *Applied Clay Science*, 105920.

Finck N., Bouby M., Dardenne K. and Yokosawa T. (2017) Yttrium co-precipitation with smectite: A polarized XAS and AsFlFFF study. *Applied Clay Science* **137**, 11–21.

Finkelman R. B., Palmer C. A. and Wang P. (2018) Quantification of the modes of occurrence of 42 elements in coal. *International Journal of Coal Geology* **185**, 138–160.

Flynn S. L., Szymanowski J. E. S. and Fein J. B. (2014) Modeling bacterial metal toxicity using a surface complexation approach. *Chemical Geology* **374–375**, 110–116.

Fowle D. A. and Fein J. B. (1999) Competitive adsorption of metal cations onto two gram positive bacteria: Testing the chemical equilibrium model. *Geochimica et Cosmochimica Acta* **63**, 3059–3067.

Franks D. M., Keenan J. and Hailu D. (2022) Mineral security essential to achieving the Sustainable Development Goals. *Nat Sustain*.

Fu B., Hower J. C., Zhang W., Luo G., Hu H. and Yao H. (2022) A review of rare earth elements and yttrium in coal ash: Content, modes of occurrences, combustion behavior, and extraction methods. *Progress in Energy and Combustion Science* **88**, 100954.

Galán E., Gómez-Ariza J. L., González I., Fernández-Caliani J. C., Morales E. and Giráldez I. (2003) Heavy metal partitioning in river sediments severely polluted by acid mine drainage in the Iberian Pyrite Belt. *Applied Geochemistry* **18**, 409–421.

Gaustad G., Williams E. and Leader A. (2021) Rare earth metals from secondary sources: Review of potential supply from waste and byproducts. *Resources, Conservation and Recycling* **167**, 105213.

Gielen D. and Lyons M. (2022) *Critical materials for the energy transition: Rare earth elements*., International Renewable Energy Agency, Abu Dhabi.

Gimeno Serrano M. J., Auqué Sanz L. F. and Nordstrom D. K. (2000) REE speciation in low-temperature acidic waters and the competitive effects of aluminum. *Chemical Geology* **165**, 167–180.

Golroudbary S. R., Makarava I., Kraslawski A. and Repo E. (2022) Global environmental cost of using rare earth elements in green energy technologies. *Science of The Total Environment* **832**, 155022.

von Gunten K., Bishop B., Plata Enriquez I., Alam M. S., Blanchard P., Robbins L. J., Feng R., Konhauser K. O. and Alessi D. S. (2019) Colloidal transport mechanisms and sequestration of U, Ni, and As in meromictic mine pit lakes. *Geochimica et Cosmochimica Acta* **265**, 292–312.

Hao W., Flynn S. L., Alessi D. S. and Konhauser K. O. (2018) Change of the point of zero net proton charge (pHPZNPC) of clay minerals with ionic strength. *Chemical Geology* **493**, 458–467.

Hao W., Flynn S. L., Kashiwabara T., Alam M. S., Bandara S., Swaren L., Robbins L. J., Alessi D. S. and Konhauser K. O. (2019) The impact of ionic strength on the proton reactivity of clay minerals. *Chemical Geology* **529**, 119294.

Hao W., Kashiwabara T., Jin R., Takahashi Y., Gingras M., Alessi D. S. and Konhauser K. O. (2020) Clay minerals as a source of cadmium to estuaries. *Sci Rep* **10**, 10417.

Hedin B. C., Hedin R. S., Capo R. C. and Stewart B. W. (2020) Critical metal recovery potential of Appalachian acid mine drainage treatment solids. *International Journal of Coal Geology* **231**, 103610.

Henderson P. ed. (1984) *Rare earth element geochemistry*., Elsevier, Amsterdam ; New York.

Herbelin A. and Westall J. (1999) FITEQL: A Computer Program for Determination of Chemical Equilibrium Constants from Experimental Data.

Hower J., Groppo J., Henke K., Hood M., Eble C., Honaker R., Zhang W. and Qian D. (2015) Notes on the Potential for the Concentration of Rare Earth Elements and Yttrium in Coal Combustion Fly Ash. *Minerals* **5**, 356–366.

Klungness G. D. and Byrne R. H. (2000) Comparative hydrolysis behavior of the rare earths and yttrium: The influence of temperature and ionic strength. *Polyhedron* **19**, 99–107.

Konhauser K. O., Hao W., Li Y., von Gunten K., Bishop B. A., Alessi D. S., Tarhan L. G., O'Connell B., Robbins L. J., Planavsky N. J. and Gingras M. K. (2020) Diopatra cuprea worm burrow parchment: a cautionary tale of infaunal surface reactivity. *Lethaia* **53**, 47–61.

Lan T., Wu P., Liu Z., Stroet M., Liao J., Chai Z., Mark A. E., Liu N. and Wang D. (2022) Understanding the Effect of pH on the Solubility and Aggregation Extent of Humic Acid in Solution by Combining Simulation and the Experiment. *Environ. Sci. Technol.* **56**, 917–927.

Lee J. H. and Byrne R. H. (1992) Examination of comparative rare earth element complexation behavior using linear free-energy relationships. *Geochimica et Cosmochimica Acta* **56**, 1127–1137.

León R., Macías F., Cánovas C. R., Pérez-López R., Ayora C., Nieto J. M. and Olías M. (2021a) Mine waters as a secondary source of rare earth elements worldwide: the case of the Iberian Pyrite Belt. *Journal of Geochemical Exploration* **224**, 106742.

León R., Macías F., R. Cánovas C., Millán-Becerro R., Pérez-López R., Ayora C. and Nieto J. M. (2023) Evidence of rare earth elements origin in acid mine drainage from the Iberian Pyrite Belt (SW Spain). *Ore Geology Reviews* **154**, 105336.

León R., Macías F., R. Cánovas C., Pérez-López R., Ayora C., Nieto J. M. and Olías M. (2021b) Mine waters as a secondary source of rare earth elements worldwide: The case of the Iberian Pyrite Belt. *Journal of Geochemical Exploration* **224**, 106742.

Lewis A. J., Komninou A., Yardley B. W. D. and Palmer M. R. (1998) Rare earth element speciation in geothermal fluids from Yellowstone National Park, Wyoming, USA. *Geochimica et Cosmochimica Acta* **62**, 657–663.

Liu H., Pourret O., Guo H. and Bonhoure J. (2017) Rare earth elements sorption to iron oxyhydroxide: Model development and application to groundwater. *Applied Geochemistry* **87**, 158–166.

Liu H., Pourret O., Guo H., Martinez R. E. and Zouhri L. (2018) Impact of hydrous manganese and ferric oxides on the behavior of aqueous rare earth elements (REE): Evidence from a modeling approach and implication for the sink of REE. *International Journal of Environmental Research and Public Health* **15**, 1–19.

Liu P., Zhao S., Xie N., Yang L., Wang Q., Wen Y., Chen H. and Tang Y. (2023) Green Approach for Rare Earth Element (REE) Recovery from Coal Fly Ash. *Environ. Sci. Technol.* **57**, 5414–5423.

Lozano A., Ayora C. and Fernández-Martínez A. (2020) Sorption of rare earth elements on schwertmannite and their mobility in acid mine drainage treatments. *Applied Geochemistry* **113**.

Lozano A., Ayora C. and Fernández-Martínez A. (2019a) Sorption of rare earth elements onto basaluminite: The role of sulfate and pH. *Geochimica et Cosmochimica Acta* **258**, 50–62.

Lozano A., Fernández-Martínez A., Ayora C., Di Tommaso D., Poulain A., Rovezzi M. and Marini C. (2019b) Solid and Aqueous Speciation of Yttrium in Passive Remediation Systems of Acid Mine Drainage. *Environ. Sci. Technol.* **53**, 11153–11161.

Luo Y. and Millero F. J. (2004) Effects of temperature and ionic strength on the stabilities of the first and second fluoride complexes of yttrium and the rare earth elements. *Geochimica et Cosmochimica Acta* **68**, 4301–4308.

Luo Y. R. and Byrne R. H. (2004) Carbonate complexation of yttrium and the rare earth elements in natural waters. *Geochimica et Cosmochimica Acta* **68**, 691–699.

Luo Y. R. and Byrne R. H. (2001) Yttrium and rare Earth element complexation by chloride ions at 25°C. *Journal of Solution Chemistry* **30**, 837–845.

Machado A., Rocha F., Gomes C., Dias J. A., Araújo M. F. and Gouveia A. (2005) Mineralogical and geochemical characterisation of surficial sediments from the Southwestern Iberian Continental Shelf. *Thalassas* **21**, 67–76.

Martinez R. E., Pourret O. and Takahashi Y. (2014) Modeling of rare earth element sorption to the Gram positive Bacillus subtilis bacteria surface. *Journal of Colloid and Interface Science* **413**, 106–111.

Miranda M. A., Ghosh A., Mahmodi G., Xie S., Shaw M., Kim S., Krzmarzick M. J., Lampert D. J. and Aichele C. P. (2022) Treatment and Recovery of High-Value Elements from Produced Water. *Water* **14**, 880.

Moldoveanu G. A. and Papangelakis V. G. (2012) Recovery of rare earth elements adsorbed on clay minerals: I. Desorption mechanism. *Hydrometallurgy* **117–118**, 71–78.

Mukai H., Kon Y., Sanematsu K., Takahashi Y. and Ito M. (2020) Microscopic analyses of weathered granite soil in ion adsorption rare earth ore of China. *Scientific Reports*, 2019.

Munemoto T., Ohmori K. and Iwatsuki T. (2014) Distribution of U and REE on colloids in granitic groundwater and quality-controlled sampling at the Mizunami underground research laboratory. *Prog. in Earth and Planet. Sci.* **1**, 28.

Ngwenya B. T., Mosselmans J. F. W., Magennis M., Atkinson K. D., Tourney J., Olive V. and Ellam R. M. (2009) Macroscopic and spectroscopic analysis of lanthanide adsorption to bacterial cells. *Geochimica et Cosmochimica Acta* **73**, 3134–3147.

Noack C. W., Dzombak D. A. and Karamalidis A. K. (2014) Rare earth element distributions and trends in natural waters with a focus on groundwater. *Environmental Science and Technology* **48**, 4317–4326.

Ohta A., Kagi H., Nomura M., Tsuno H. and Kawabe I. (2009) Coordination study of rare earth elements on Fe oxyhydroxide and Mn dioxides: Part I. Influence of a multi-electron excitation on EXAFS analyses of La, Pr, Nd, and Sm. *American Mineralogist* **94**, 467–475.

Olías M., Cánovas C. R., Basallote M. D. and Lozano A. (2018) Geochemical behaviour of rare earth elements (REE) along a river reach receiving inputs of acid mine drainage. *Chemical Geology* **493**, 468–477.

Pan J., Zhou C., Tang M., Cao S., Liu C., Zhang N., Wen M., Luo Y., Hu T. and Ji W. (2019) Study on the modes of occurrence of rare earth elements in coal fly ash by statistics and a sequential chemical extraction procedure. *Fuel* **237**, 555–565.

Pawar G. and Ewing R. C. (2022) Recent advances in the global rare-earth supply chain. *MRS Bulletin* **47**, 244–249.

Pourret O. and Davranche M. (2013) Rare earth element sorption onto hydrous manganese oxide: A modeling study. *Journal of Colloid and Interface Science* **395**, 18–23.

Pourret O., Davranche M., Gruau G. and Dia A. (2007) Rare earth elements complexation with humic acid. *Chemical Geology* **243**, 128–141.

Quillinan S., Nye C., Engle M., Bartos T., Brant J., Bagdonas D., McLing T. and McLaughlin J. F. (2018) *Assessing rare earth element concentrations in geothermal and oil and gas produced waters: A potential domestic source of strategic mineral commodities*., US Department of Energy.

Ravel B. (2001) *ATOMS* : crystallography for the X-ray absorption spectroscopist. *J Synchrotron Rad* **8**, 314–316.

Ravel B. and Newville M. (2005) *ATHENA* , *ARTEMIS* , *HEPHAESTUS* : data analysis for X-ray absorption spectroscopy using *IFEFFIT*. *J Synchrotron Rad* **12**, 537–541.

Rehr J. J. and Albers R. C. (2000) Theoretical approaches to x-ray absorption fine structure. *Rev. Mod. Phys.* **72**, 621–654.

Ressler T. (1997) WinXAS. In *Journal de Physique IV* Internation Conference on X-Ray Absorption Fine Structure (XAFS IX). EDP Sciences, Grenoble, France. p. C2.269-C2.270.

Rivera N., Kaur N., Hesterberg D., Ward C. R., Austin R. E. and Duckworth O. W. (2015) Chemical Composition, Speciation, and Elemental Associations in Coal Fly Ash Samples Related to the Kingston Ash Spill. *Energy Fuels* **29**, 954–967.

Roth E., Bank T., Howard B. and Granite E. (2017) Rare Earth Elements in Alberta Oil Sand Process Streams. *Energy and Fuels* **31**, 4714–4720.

Royer-Lavallée A., Neculita C. M. and Coudert L. (2020) Removal and potential recovery of rare earth elements from mine water. *Journal of Industrial and Engineering Chemistry* **89**, 47–57.

Sánchez España J. (2007) The Behavior of Iron and Aluminum in Acid Mine Drainage: Speciation, Mineralogy, and Environmental Significance. In *Thermodynamics, Solubility and Environmental Issues* Elsevier. pp. 137–150.

Sanematsu K. and Watanabe Y. (2016) Characteristics and Genesis of Ion Adsorption-Type Rare Earth Element Deposits. In *Rare Earth and Critical Elements in Ore Deposits* Society of Economic Geologists.

Schad M., Halama M., Bishop B., Konhauser K. O. and Kappler A. (2019) Temperature fluctuations in the Archean ocean as trigger for varve-like deposition of iron and silica minerals in banded iron formations. *Geochimica et Cosmochimica Acta* **265**, 386–412.

Schijf J. and Byrne R. H. (2004) Determination of SO4β1 for yttrium and the rare earth elements at I = 0.66 m and t = 25°C-implications for YREE solution speciation in sulfate-rich waters. *Geochimica et Cosmochimica Acta* **68**, 2825–2837.

Seredin V. V. and Dai S. (2012) Coal deposits as potential alternative sources for lanthanides and yttrium. *International Journal of Coal Geology* **94**, 67–93.

Seredin V. V., Dai S., Sun Y. and Chekryzhov I. Yu. (2013) Coal deposits as promising sources of rare metals for alternative power and energy-efficient technologies. *Applied Geochemistry* **31**, 1–11.

Smith Y., Kumar P. and McLennan J. (2017) On the Extraction of Rare Earth Elements from Geothermal Brines. *Resources* **6**, 39.

Sposito G., Skipper N. T., Sutton R., Park S. H., Soper A. K. and Greathouse J. A. (1999) Surface geochemistry of the clay minerals. *Proceedings of the National Academy of Sciences of the United States of America* **96**, 3358–3364.

Stewart B. W., Capo R. C., Hedin B. C. and Hedin R. S. (2017) Rare earth element resources in coal mine drainage and treatment precipitates in the Appalachian Basin, USA. *International Journal of Coal Geology* **169**, 28–39.

Stoy L., Diaz V. and Huang C.-H. (2021) Preferential Recovery of Rare-Earth Elements from Coal Fly Ash Using a Recyclable Ionic Liquid. *Environ. Sci. Technol.* **55**, 9209–9220.

Stumpf T., Bauer A., Coppin F., Fanghänel T. and Kim J.-I. (2002) Inner-sphere, outer-sphere and ternary surface complexes: a TRLFS study of the sorption process of Eu(III) onto smectite and kaolinite. *Radiochimica Acta* **90**, 345–349.

Stumpf T., Curtius H., Walther C., Dardenne K., Ufer K. and Fanghänel T. (2007) Incorporation of Eu(III) into Hydrotalcite: A TRLFS and EXAFS Study. *Environ. Sci. Technol.* **41**, 3186–3191.

Tian L., Shi Z., Lu Y., Dohnalkova A., Lin Z. and Dang Z. (2017) Kinetics of Cation and Oxyanion Adsorption and Desorption on Ferrihydrite: Roles of Ferrihydrite Binding Sites and a Unified Model. *Environmental Science & Technology*, acs.est.7b03249.

Tonkin J. W., Balistrieri L. S. and Murray J. W. (2004) Modeling sorption of divalent metal cations on hydrous manganese oxide using the diffuse double layer model. *Applied Geochemistry* **19**, 29–53.

Vass C. R., Noble A. and Ziemkiewicz P. F. (2019a) The occurrence and concentration of rare earth elements in acid mine drainage and treatment byproducts: Part 1 - Initial survey of the northern Appalachian Coal Basin. *Mining Engineering* **71**, 49–50.

Vass C. R., Noble A. and Ziemkiewicz P. F. (2019b) The occurrence and concentration of rare earth elements in acid mine drainage and treatment byproducts: Part 2: Regional survey of Northern and Central Appalachian coal basins. *Mining Engineering* **36**, 917–929.

Verplanck P. L., Nordstrom D. K., Taylor H. E. and Kimball B. A. (2004) Rare earth element partitioning between hydrous ferric oxides and acid mine water during iron oxidation. *Applied Geochemistry* **19**, 1339–1354.

Viers J., Dupré B. and Gaillardet J. (2009) Chemical composition of suspended sediments in World Rivers: New insights from a new database. *Science of the Total Environment* **407**, 853–868.

Wang Xiaomei, Wang Xiaoming, Pan Z., Yin X., Chai P., Pan S. and Yang Q. (2019) Abundance and distribution pattern of rare earth elements and yttrium in vitrain band of high-rank coal from the Qinshui basin, northern China. *Fuel* **248**, 93–103.

Warchola T. J., Flynn S. L., Robbins L. J., Liu Y., Gauger T., Kovalchuk O., Alam M. S., Wei S., Myers R., Bishop B., Lalonde S. V., Gingras M. K., Kappler A., Alessi D. S. and Konhauser K. O. (2017) Field- and Lab-Based Potentiometric Titrations of Microbial Mats from the Fairmont Hot Spring, Canada. *Geomicrobiology Journal* **34**, 851–863.

Yin X., Martineau C., Demers I., Basiliko N. and Fenton N. J. (2021) The potential environmental risks associated with the development of rare earth element production in Canada. *Environ. Rev.* **29**, 354–377.

Zhang Y., Tan H., Zhang W., Wei H. and Dong T. (2016) Geochemical constraint on origin and evolution of solutes in geothermal springs in western Yunnan, China. *Chemie der Erde* **76**, 63–75.